

# Structural and Functional Studies of Ig $\alpha$ $\beta$ and Its Assembly with the B Cell Antigen Receptor

Sergei Radaev,<sup>1</sup> Zhongcheng Zou,<sup>1</sup> Pavel Tolar,<sup>2</sup> Khanh Nguyen,<sup>1</sup> AnhThao Nguyen,<sup>1</sup> Peter D. Krueger,<sup>2</sup> Nicole Stutzman,<sup>1</sup> Susan Pierce,<sup>2</sup> and Peter D. Sun<sup>1,\*</sup>

<sup>1</sup>Structural Immunology Section

<sup>2</sup>Lymphocyte Activation Section

Laboratory of Immunogenetics, National Institute of Allergy and Infectious Diseases, National Institutes of Health, 12441 Parklawn Drive, Rockville, MD 20852, USA

\*Correspondence: [psun@nih.gov](mailto:psun@nih.gov)

DOI 10.1016/j.str.2010.04.019

## SUMMARY

The B cell antigen receptor (BCR) plays an essential role in all phases of B cell development. Here we show that the extracellular domains of murine and human Ig $\beta$  form an I-set immunoglobulin-like structure with an interchain disulfide between cysteines on their G strands. Structural and sequence analysis suggests that Ig $\alpha$  displays a similar fold as Ig $\beta$ . An Ig $\alpha$  $\beta$  heterodimer model was generated based on the unique disulfide-bonded Ig $\beta$  dimer. Solution binding studies showed that the extracellular domains of Ig $\alpha$  $\beta$  preferentially recognize the constant region of BCR with  $\mu$  chain specificity, suggesting a role for Ig $\alpha$  $\beta$  to enhance BCR $\mu$  chain signaling. Cluster mutations on Ig $\alpha$ , Ig $\beta$ , and a membrane-bound form of immunoglobulin (mIgM) based on the structural model identified distinct areas of potential contacts involving charged residues on both subunits of the coreceptor and the C $\mu$ 4 domain of mIgM. These studies provide the first structural model for understanding BCR function.

## INTRODUCTION

The B cell antigen receptor (BCR) plays a critical role in all stages of B cell development and function (Geisberger et al., 2006; Reth, 1992). It consists of two principal components: an antigen binding subunit and a signaling subunit. The antigen binding subunit is a membrane-bound form of immunoglobulin (mIg) with a short cytoplasmic tail lacking any signaling motifs. Through noncovalent interactions, mIg associates with a disulfide-linked Ig $\alpha$  $\beta$  (CD79a/CD79b) signaling heterodimer (Campbell et al., 1991; Hermanson et al., 1988; Kashiwamura et al., 1990; Venkitaraman et al., 1991), forming a complex with 1:1 stoichiometry (Schamel and Reth, 2000; Tolar et al., 2005). Both Ig $\alpha$  and Ig $\beta$  contain a single immunoreceptor tyrosine-based activation motif (ITAM) in their cytoplasmic domains (Cambier, 1995; Reth, 1989). Upon antigen binding, the ITAMs of Ig $\alpha$  and Ig $\beta$  are phosphorylated by the Src-family kinase Lyn, initiating a signaling cascade in B cells (Dal Porto et al., 2004; Gauld et al., 2002;

Jumaa et al., 2005). Importantly, both positive and negative selection of developing B lymphocytes as well as the survival and activation of mature B cells depend critically on Ig $\alpha$  and Ig $\beta$  (Nemazee et al., 2000; Rajewsky, 1996). It was also established that mIgM is absolutely dependent on the association with Ig $\alpha$  $\beta$  heterodimer for its cell-surface expression, whereas mIgG1 is not (Venkitaraman et al., 1991).

A critical gap in our knowledge of how the BCRs transduce signals is the molecular architecture of mIg-Ig $\alpha$  $\beta$  complex. It is well established that many multichain immune receptors, such as T cell receptors (TCRs) and activating natural killer cell receptors, associate with their signaling adaptor molecules through interactions between positively and negatively charged amino acid pairs in their transmembrane (TM) domains (Lanier, 2005). For the BCR, only Ig $\alpha$  has a charged residue in its transmembrane domain, and mIgM and Ig $\beta$  contain only two polar residues in their TM regions (Campbell et al., 1991; Reth, 1992). The presence of a charged Glu residue in the TM portion of Ig $\alpha$  led to the hypothesis that interactions between mIgM and the Ig $\alpha$  $\beta$  heterodimer are primarily through Ig $\alpha$  (Reth, 1992). However, recent studies utilizing fluorescence resonance energy transfer (FRET) have demonstrated that the cytoplasmic C terminus of Ig $\beta$  is positioned closer to mIg than Ig $\alpha$  (Tolar et al., 2005; Wienands, 2005). Mutational studies confirmed a critical role for polar residues in the transmembrane region of mIgM and revealed that YS to VV mutation in the TM region of  $\mu$  chain abolishes its association with Ig $\alpha$  $\beta$  heterodimer (Grupp et al., 1993). Later experiments proposed that there is an ordered association of BCR components during BCR assembly (Foy and Matsuuchi, 2001). An intriguing aspect of the BCR signaling subunit is its structural and functional similarity to CD3 molecules in TCR assembly. Unlike many signaling subunits in immune receptors that do not have appreciable extracellular domains, Ig $\alpha$  and Ig $\beta$  have sizable extracellular domains, as do CD3 $\delta\epsilon$  or CD3 $\gamma\epsilon$  heterodimers in TCRs (Call et al., 2002; Clevers et al., 1988; Kuhns et al., 2006; Wegener et al., 1995). However, unlike Ig $\alpha$  $\beta$ , CD3 $\delta\epsilon$  and CD3 $\gamma\epsilon$  are not disulfide-bonded heterodimers.

The exact role of extracellular domains of Ig $\alpha$  $\beta$  in BCR assembly and signaling remains unresolved. It was reported that the extracellular domain of Ig $\alpha$  affects the expression level of mIgM (Hombach et al., 1990). Moreover, Ig $\alpha$  and Ig $\beta$  that lack extracellular domains did not mediate transport of IgM to the B cell surface (Alfarano et al., 1999; Indraccolo et al., 2002). Recently, it was also reported that both extracellular and

transmembrane regions of Ig $\alpha\beta$  must be properly associated for correct BCR assembly (Dylke et al., 2007). It is also interesting to note that an excess of Ig $\beta$  has been observed in the endoplasmic reticulum of B cells as a disulfide-bonded homodimer, although its functional relevance is uncertain (Brouns et al., 1995; Schamel et al., 2003). Based on amino acid sequences, the extracellular domains of Ig $\alpha$  and Ig $\beta$  are predicted to have a C2- and a V-set immunoglobulin-like (Ig-like) fold, respectively (Hermanson et al., 1988; Kashiwamura et al., 1990). In addition to the classical Ig-fold intrachain disulfide bond, both Ig $\alpha$  and Ig $\beta$  contain additional cysteines that form an interchain heterodimeric disulfide bond. Ig $\beta$  also has an additional intramolecular disulfide bond. At present, the cysteine assignment for the intra- and intermolecular disulfide bonds in Ig $\beta$  remains controversial (Campbell et al., 1991; Hermanson et al., 1988; Kashiwamura et al., 1990; Reth, 1992; Siegers et al., 2006). To further investigate the function of Ig $\alpha\beta$  and its association with BCR, we determined crystal structures of the extracellular domains of murine and human Ig $\beta$ , generated a structural model for Ig $\alpha\beta$ , carried out solution binding studies between Ig $\alpha\beta$  and various isotypes of the B cell receptors, and identified, through mutational analysis, residues on the extracellular portion of Ig $\alpha\beta$  as well as in the C $\mu$ 4 domain of mIgM involved in the receptor and coreceptor association. Together, these studies provide the first structural model for our understanding of BCR architecture and activation.

## RESULTS AND DISCUSSION

### The Extracellular Domains of Ig $\alpha$ and Ig $\beta$ Preferentially Recognize BCR $\mu$ Chain

In addition to mediating BCR signaling, Ig $\alpha\beta$  promotes the surface expression of mlg heavy chains, in particular the  $\mu$  chain of BCR (Venkitaraman et al., 1991). In the absence of Ig $\alpha\beta$ ,  $\mu$  chain of BCR is retained in the endoplasmic reticulum (ER) through interactions of its TM domain with calnexin (Grupp et al., 1995). The association between Ig $\alpha\beta$  and mlg has been probed extensively through mutations in the TM region of mlg and pinpointed to a Tyr-Ser pair of amino acids (Blum et al., 1993; Grupp et al., 1993; Pleiman et al., 1994; Venkitaraman et al., 1991; Williams et al., 1994). The results showed that Ig $\alpha\beta$  interacts with mlg primarily through its TM regions and that the extracellular domains of Ig $\alpha\beta$  appear to be dispensable for BCR signaling. However, the interactions between Ig $\alpha\beta$  and mlg in the TM region alone are insufficient to explain the ER retention of  $\mu$  chain but not  $\gamma$  chain of mlg, as they share 70% similar TM sequences with the Tyr-Ser pair conserved for all mlg isotypes.

To investigate the function of the extracellular region of Ig $\alpha\beta$ , we examined the binding of soluble Ig $\alpha\beta$  to different Ig isotypes, including IgM, IgG $_1$ , IgD, IgA, and IgE. Human Ig $\alpha\beta$  heterodimer was expressed in insect cells as a leucine zipper fusion protein (Ig $\alpha\beta$ -LZ). The constant portion of a human BCR  $\mu$  chain, corresponding to C $\mu$ 2–C $\mu$ 4 domains (Fc $\mu$ ), was expressed in CHO cells as a disulfide-bonded dimer and reacted with an anti-human IgM antibody. The solution binding experiments were carried out using immobilized human Ig $\alpha\beta$ -LZ on CM5 sensor chips via primary amine attachment. The analytes consisted of serial dilutions of recombinant human Fc $\mu$  and human IgM, IgA, IgD, IgE, and IgG $_1$ . The solution binding showed that Ig $\alpha\beta$  bound Fc $\mu$  tightest, with a dissociation constant of  $\sim 2$   $\mu$ M (Figure 1

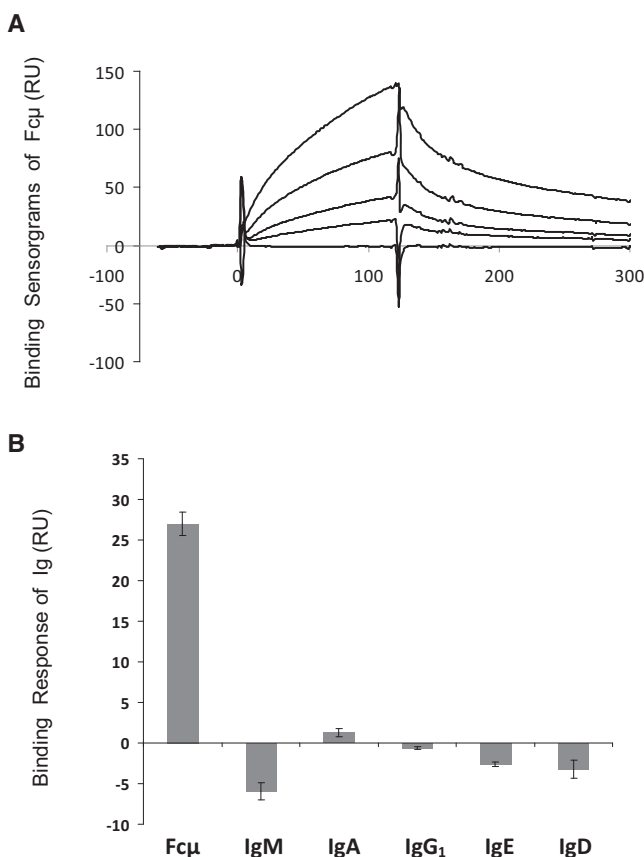


**Figure 1. Solution Binding of Immunoglobulins to Immobilized Ig $\alpha\beta$  at 540 RU of Surface Densities**

(A) The binding sensorgrams of recombinant Fc $\mu$  at 10, 5, 2.5, 1.25, and 0.625  $\mu$ M concentrations to immobilized Ig $\alpha\beta$ . The calculated dissociation constant  $K_D$  is  $2.3 \times 10^{-6} \pm 1.1 \times 10^{-6}$   $\mu$ M.

(B) The binding responses of 3  $\mu$ M Fc $\mu$  and various human immunoglobulins to immobilized Ig $\alpha\beta$ . The responses were taken at the time point immediately before the dissociation phase. The average and their standard deviations are derived from three independent experiments.

and Table 1). Interestingly, the intact IgM bound Ig $\alpha\beta$  significantly less than Fc $\mu$  despite its being 10 $\times$  larger than Fc $\mu$  (Table 1), suggesting that the presence of J chain on IgM interferes with Ig $\alpha\beta$  binding. Similarly, IgA displayed weak binding to Ig $\alpha\beta$  at a high level of coreceptor immobilization and failed to bind the coreceptor at low immobilization levels (Table 1). No binding was observed between IgG $_1$ , IgD, IgE, and immobilized Ig $\alpha\beta$  under any surface densities. Thus, the solution binding results showed a preferential  $\mu$  chain association by the extracellular domains of Ig $\alpha\beta$ , suggesting a unique role for the coreceptor in enhancing BCR $\mu$  signaling. This may contribute to lowering the signaling threshold of the receptor and compensate for the lower  $\mu$  chain antigen affinity during B cell development.

### Structure Determination of Murine and Human Ig $\beta$

To gain structural insights into the signaling chain of BCR, we expressed the extracellular portions of human Ig $\alpha$  (amino acids 33–143), Ig $\beta$  (amino acids 26–159), as well as their murine homologs as recombinant proteins in *Escherichia coli*. The refolded

**Table 1. Solution Affinities of Fcμ and Immunoglobulins Binding to Igαβ**

	Igαβ			
Immobilization (RU)	250	540	990	2096
Analyte (concentrations)	Dissociation Constants, K <sub>D</sub> (μM)			
Fcμ (0–20 μM)	2.4 ± 2.9	2.3 ± 1.1	2.2 ± 2.2	0.9
IgM (0–20 μM)	ND	ND	ND	>10
IgA (0–20 μM)	ND	ND	ND	>10
IgG1 (0–6 μM)	ND	ND	ND	ND
IgE (0–6 μM)	ND	ND	ND	ND
IgD (0–6 μM)	ND	ND	ND	ND

ND, nondetectable binding.

human Igα existed in mostly a monomeric form, whereas human and murine Igβ formed both monomers and dimers (see Figure S1 available online). Both Igα and Igβ, when immobilized on a CM5 sensor chip, bound Fcμ as well as their respective antibodies, suggesting that the refolded Igα and Igβ were functional. We crystallized the monomeric and dimeric forms of murine Igβ as well as the dimeric form of human Igβ. The crystals of the monomeric Igβ belonged to an orthorhombic space group *P*2<sub>1</sub>2<sub>1</sub>2 and contained one Igβ monomer in each asymmetric unit. The structure was determined by the molecular replacement method despite less than 30% sequence identity between Igβ and the known structures of V-set Ig-like domains. The structure was refined to 1.7 Å resolution with crystallographic and free R factors of R<sub>cryst</sub> = 18.7% and R<sub>free</sub> = 19.7%, respectively (Table 2). The refined electron density map was contiguous from residue Cys43 to Leu142 except for the FG loop, between residues 127 and 133, which appeared disordered (Figure S2). The refined monomeric Igβ structure was then used as the search model in molecular replacement to solve both murine and human dimeric Igβ structures (Table 2). The structure of the murine Igβ dimer was refined to 3.1 Å resolution with a final R<sub>cryst</sub> and R<sub>free</sub> of 20.6% and 25.8%, respectively. The electron densities are continuous between Cys43 and Leu142 for the A subunit except for the FG loop (residues 125–129), and between Ile46 and Phe144 for the B subunit except for part of the C'D (residues 90–91) and FG (residues 124–132) loops. The dimeric human Igβ structure was refined to 3.2 Å resolution with a final R<sub>cryst</sub> and R<sub>free</sub> of 18.1% and 26.3%, respectively (Table 2 and Figures 2 and 3). The refined (2F<sub>o</sub> – F<sub>c</sub>) map showed good electron density in both subunits throughout the whole structure between Cys43 and Phe145.

The subunit structures of murine and human Igβ are very similar to one another, with a root-mean-square deviation (rmsd) of 1.2 Å among 86 core Cα atoms (Figure 2C). The overall structure of the Igβ extracellular domain assumes an I-type Ig fold with the two antiparallel β sheets formed by A-B-E-D and A'-G-F-C strands and a characteristic disulfide bond between Cys65 and Cys120 (Cys122 in human Igβ) from the B and F strands, respectively (Figure 2) (Harpaz and Chothia, 1994). Like a V-type fold, a conserved proline residue, Pro50, breaks the first β strand into two shorter strands, A and A'. However, unlike the classical V-type domain, the I-type Igβ does not have a C'' β strand, leaving C' strand to bridge the two β sheets (Figure 2). As a consequence, the loop corresponding to the

**Table 2. Data Collection and Refinement Statistics**

	Murine Igβ Monomer	Murine Igβ Homodimer	Human Igβ Homodimer
Data Collection			
Space group	<i>P</i> 2 <sub>1</sub> 2 <sub>1</sub> 2	<i>P</i> 4 <sub>1</sub> 2 <sub>1</sub> 2	<i>P</i> 4 <sub>1</sub> 32
Unit cell (Å)	<i>a</i> = 35.63, <i>b</i> = 79.72, <i>c</i> = 34.32	<i>a</i> = <i>b</i> = 87.97, <i>c</i> = 75.29	<i>a</i> = 129.83
Resolution limit (Å)	1.7	3.1	3.2
Unique reflections	10,471 (898) <sup>a</sup>	5,597 (541)	6,616 (630)
Redundancy	5.5 (2.3)	6.1 (5.4)	27.6 (28.7)
Completeness (%)	93.8 (67.4)	97.4 (98.7)	99.9 (100.0)
R <sub>sym</sub> (%) <sup>b</sup>	6.5 (31.7)	13.5 (50.6)	7.0 (33.9)
<I/σ(I)>	21.5 (2.6)	14.1 (3.2)	55.6 (13.1)
Refinement			
Resolution (Å)	40–1.7	48–3.1	46–3.2
Number of reflections	10,071	5,407	6,407
Number of protein atoms	757	1,485	1,678
Number of solvent atoms	92	26	2
R <sub>cryst</sub> (%)	18.7 (27.0)	20.6 (27.8)	18.1 (20.7)
R <sub>free</sub> (%) <sup>c</sup>	19.7 (29.0)	25.8 (32.0)	26.3 (36.2)
Mean B factor (Å <sup>2</sup> )	31.7	52.1	77.2
Wilson B factor (Å <sup>2</sup> )	20.6	59.7	75.8
Rmsd bond lengths (Å)	0.006	0.007	0.010
Rmsd bond angles (°)	1.18	1.39	1.39

<sup>a</sup>Values in parentheses are for highest resolution shells: 1.7–1.74 Å, 3.21–3.10 Å, and 3.31–3.20 Å for murine Igβ monomer, murine Igβ homodimer, and human Igβ homodimer, respectively.

<sup>b</sup>R<sub>sym</sub> = 100 × Σ|I<sub>h</sub> – <I<sub>h</sub>>|/ΣI<sub>h</sub>, where <I<sub>h</sub>> is the mean intensity of multiple measurements of symmetry-equivalent reflections.

<sup>c</sup>R<sub>free</sub> was calculated using a test set of 5%.

putative second complementarity-determining region (CDR2) is absent in Igβ. The structural comparison between Igβ and several other members of the Ig superfamily such as the V<sub>H</sub> and V<sub>L</sub> domains of an IgG1 (Protein Data Bank [PDB] ID code 1YQV), the Vα and Vβ domains of a TCR (1AO7), the Vγ and Vδ domains of a γδTCR (1HXM), and CD8 (1CD8) resulted in rmsds of 1.1–1.3 Å for 75–87 Cα atoms. In addition, Igβ contains a second intrachain disulfide bond formed between Cys43 and Cys124 (Cys126 in human Igβ), and an interchain disulfide bond between Cys135 (Cys136 in human Igβ) from both subunits (Figure 3). Our structural data are in accordance with the reported Igαβ heterodimer formation through Cys135 of murine Igβ in *Drosophila* S2 cells (Siegers et al., 2006).

### Igβ Forms a Distinct Dimer

Although its functional relevance is unclear, an excess of Igβ could be found in B cells as a disulfide-bonded homodimer (Brouns et al., 1995; Schamel et al., 2003). The two subunits of Igβ are linked by a disulfide bond between Cys135 (Cys136 in

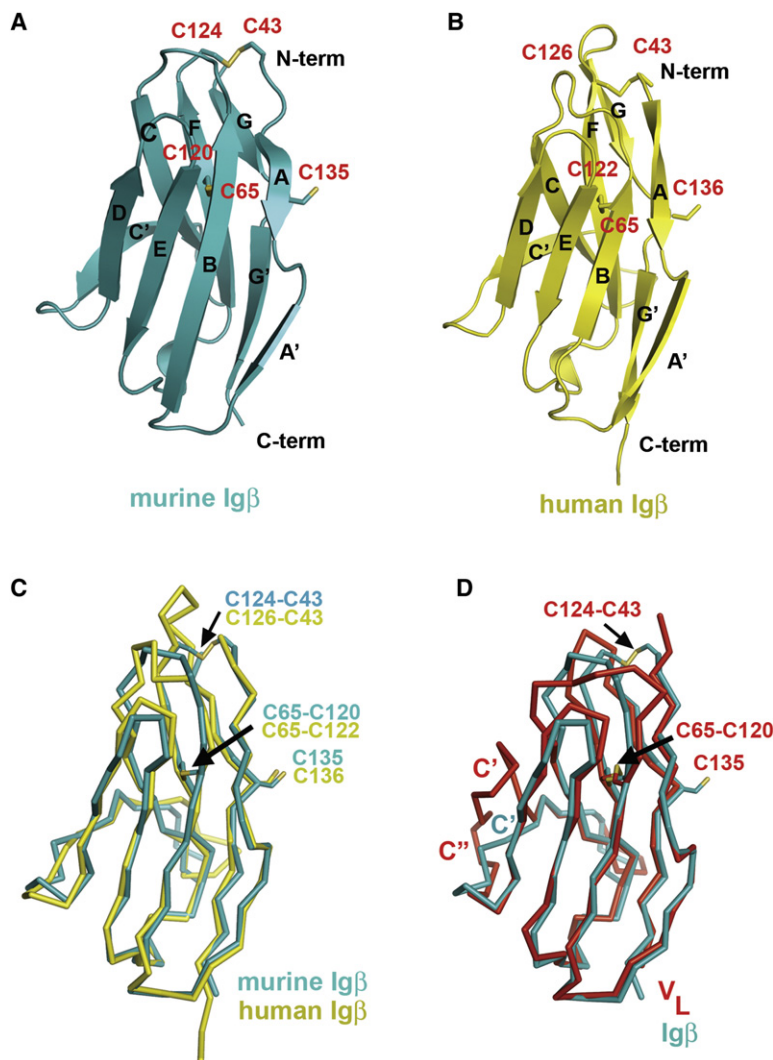


**Figure 2. The Structure of Murine and Human Ig $\beta$**

(A and B) Monomers from murine (A) and human (B) Ig $\beta$  homodimers are shown with their secondary-structure elements labeled as in Figure 4. Cysteines (labeled in red) and disulfide bonds are shown in stick representation. N and C termini are marked.

(C) Structural comparison between murine Ig $\beta$  (cyan) and human Ig $\beta$  (yellow) monomers. Positions of disulfide bonds are shown with arrows. Labels are colored according to the color of the corresponding molecule.

(D) Structural comparison between murine Ig $\beta$  (cyan) and V<sub>L</sub> domain of IgG1 (red, PDB ID code 1YQV). Cysteines and disulfide bonds are shown in stick representation, labeled according to the Ig $\beta$  sequence. C' and C'' strands, which are different in the two structures, are labeled and colored according to the color of the corresponding molecule. This figure and all subsequent ribbon drawings are prepared using the program PyMOL (<http://www.pymol.org>). See also Figure S2.

human Ig $\beta$ ) from the opposing G strands (Figure 3). Unlike many covalent dimers, such as CD8, NKG2D, and NKG2A/CD94 receptors, that usually form disulfide bonds in their membrane proximal stalk regions, the Ig $\beta$  intersubunit disulfide bond is located in the middle of its Ig domain. Similar to the V domain structures of antibodies and T cell receptors, the structure of Ig $\beta$  contains a glycine residue, Gly136 (Gly137 in human Ig $\beta$ ), in the middle of the G strand, creating a  $\beta$  bulge that splits the strand into G and G' strands (Chothia, et al., 1998; Richardson, 1981). Interestingly, Cys135 (Cys136 in human Ig $\beta$ ) is located in the middle of the bulge, whose conformation makes the cysteine readily accessible for the interchain disulfide-bond formation (Figures 2 and 3). Although similar in overall dimer formation, the relative orientations of two Ig $\beta$  subunits differ between the murine and human homodimers as a result of a rotation around the interchain disulfide bond (Figures 3A and 3C). The murine dimer is asymmetrical and stabilized by interactions between subunits A and B, including two salt bridges (Lys78 [A]–Glu138 [B] and Asp133 [A]–His49 [B]), one hydrogen bond (Asn130 [A]–Tyr66 [B]), and hydrophobic interactions involving

Ile117 (A), Phe119 (A), Gln45 (A), Lys78 (A), Trp47 (B), and Phe52 (B) (Figures 3A and 3B). In contrast, the human Ig $\beta$  homodimer is symmetrical and primarily formed through hydrogen bonds from the side chains of Arg45 and Arg51 to the main-chain atoms of the opposing subunit (Figures 3C and 3D). In addition to the current Ig $\beta$ -type dimer, several types of immunoglobulin dimers have been reported to date, including those in the V domains of antibodies, TCRs, CD8, CTLA-4, CD28, and TREM-1 (Cohen et al., 1996; Evans et al., 2005; Garboczi et al., 1996; Harris et al., 1992; Leahy et al., 1992; Ostrov et al., 2000; Radaev et al., 2003; Schwartz et al., 2001) (Figure S3). However, all these reported dimers would position the interchain cysteines of Ig $\beta$  at distances between 12 and 25 Å, too far for disulfide-bond formation, and thus are incompatible with the Ig $\alpha\beta$  structure.

Based on initial sequence analysis, Ig $\alpha$  was proposed to have a C2-set Ig-like fold (Kashiwamura et al., 1990). The sequences of Ig $\alpha$  and Ig $\beta$  share less than 20% identity (Figure 4). However, several structural features of Ig $\beta$  appear to also be present in the structure of Ig $\alpha$ . First, a conserved Pro35 in the first  $\beta$  strand of Ig $\alpha$  suggests its first strand is split into A and A' strands, like those in the V-type and I-type Ig fold. Second, the most conserved region between Ig $\alpha$  and Ig $\beta$  (~60% of sequence identity) corresponds to the GG'  $\beta$  bulge and the G' strand of Ig $\beta$  (Figure 4B). In particular, the four residues at the  $\beta$  bulge of Ig $\beta$  (SCGT) are invariant in all Ig $\alpha$  sequences (Figure 4C), suggesting that the  $\beta$  bulge conformation of Ig $\beta$  is also present in the structure of Ig $\alpha$ . This, together with the conserved Pro35 in Ig $\alpha$  sequences, likely creates A' and G' strand pairing in Ig $\alpha$  that is similar to that of Ig $\beta$ . The interchain disulfide-forming cysteine, Cys113 of Ig $\alpha$ , is aligned against the dimer-forming cysteine 135 of murine Ig $\beta$  (Figure 4B), suggesting that the heterodimeric disulfide bond is formed between Cys113 of Ig $\alpha$  and Cys135 of Ig $\beta$  (murine numbering). The sequence of Ig $\alpha$  is also compatible with the hydrogen bonding observed in the structure of



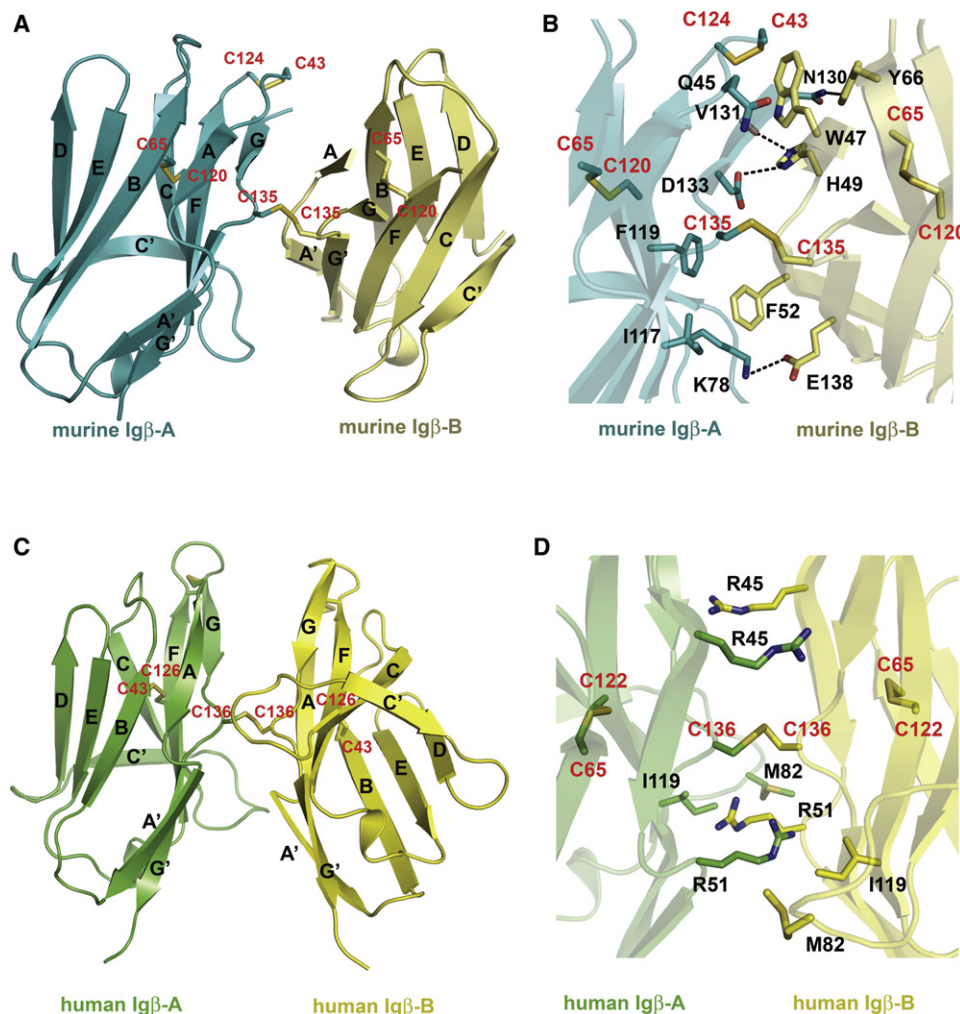


**Figure 3. Murine and Human Ig $\beta$  Homodimer Formation**

(A) Murine Ig $\beta$  homodimer with secondary-structure elements labeled. Monomers A and B are colored cyan and lemon, respectively. (B) Detailed view of the hydrophobic core and hydrogen bonds (black dashed lines) at the homodimer interface with major side chains involved in the interactions. (C) Human Ig $\beta$  homodimer. Monomers A and B are colored green and yellow, respectively. (D) Detailed view of major side chains involved in the interactions at the human Ig $\beta$  interface. Cysteine residues are shown in stick representation and labeled red. See also Figure S3.

asymmetric murine Ig $\beta$  dimer (Figure S4). Because the dimerization mode observed in Ig $\beta$  is the only one compatible with the interchain disulfide bond through the GG'  $\beta$  bulge cysteines, we modeled the structure of Ig $\alpha\beta$  heterodimer based on that of the asymmetric murine Ig $\beta$  dimer (Figure S4).

#### Identification of the Contact Regions between Ig $\alpha\beta$ and the $\mu$ Chain of BCR

The structure model of Ig $\alpha\beta$  reveals approximately nine polar and charged patches on the surface of the heterodimer. To further define the contact region between  $\mu$  chain of BCR and Ig $\alpha\beta$ , we carried out cluster mutagenesis on both subunits of Ig $\alpha\beta$  heterodimer as well as the  $\mu$  chain of BCR. Cluster mutations, in which clusters of amino acids are replaced with alanines, generally result in larger effects than single alanine mutations and can be effectively used to map a ligand binding

site. However, a potential complication of cluster mutations is their higher tendency to disrupt native conformations. Thus, the approach requires conformational-sensitive validations, such as antibody binding. Based on the human Ig $\alpha\beta$  model, two surface-exposed Ig $\alpha$  clusters, E48/D49/H51 ( $\alpha$ 2) and R124/V125/R126 ( $\alpha$ 5), together with three individual amino acid sites, H36 ( $\alpha$ 1), N60 ( $\alpha$ 3), and E85 ( $\alpha$ 4), were selected for alanine mutations (Figure 5). Four Ig $\beta$  clusters, R55A/K56A/R57A ( $\beta$ 1), T60A/V61A/K62A ( $\beta$ 2), K79A/Q80A/E81A ( $\beta$ 3), and Q123A/Q124A/K125A ( $\beta$ 4), were also generated. The mutations were carried out on Ig $\alpha$  and Ig $\beta$  subunits to avoid mutations affecting Ig $\alpha\beta$  heterodimer formation which would complicate the mapping of the BCR binding site. Seven out of nine mutants were successfully expressed in *E. coli* and refolded in vitro. Two mutants, E48A/D49A/H51A ( $\alpha$ 2) of Ig $\alpha$  and T60A/V61A/K62A ( $\beta$ 2) of Ig $\beta$ , failed to express. The refolded Ig $\alpha$  and Ig $\beta$  mutants

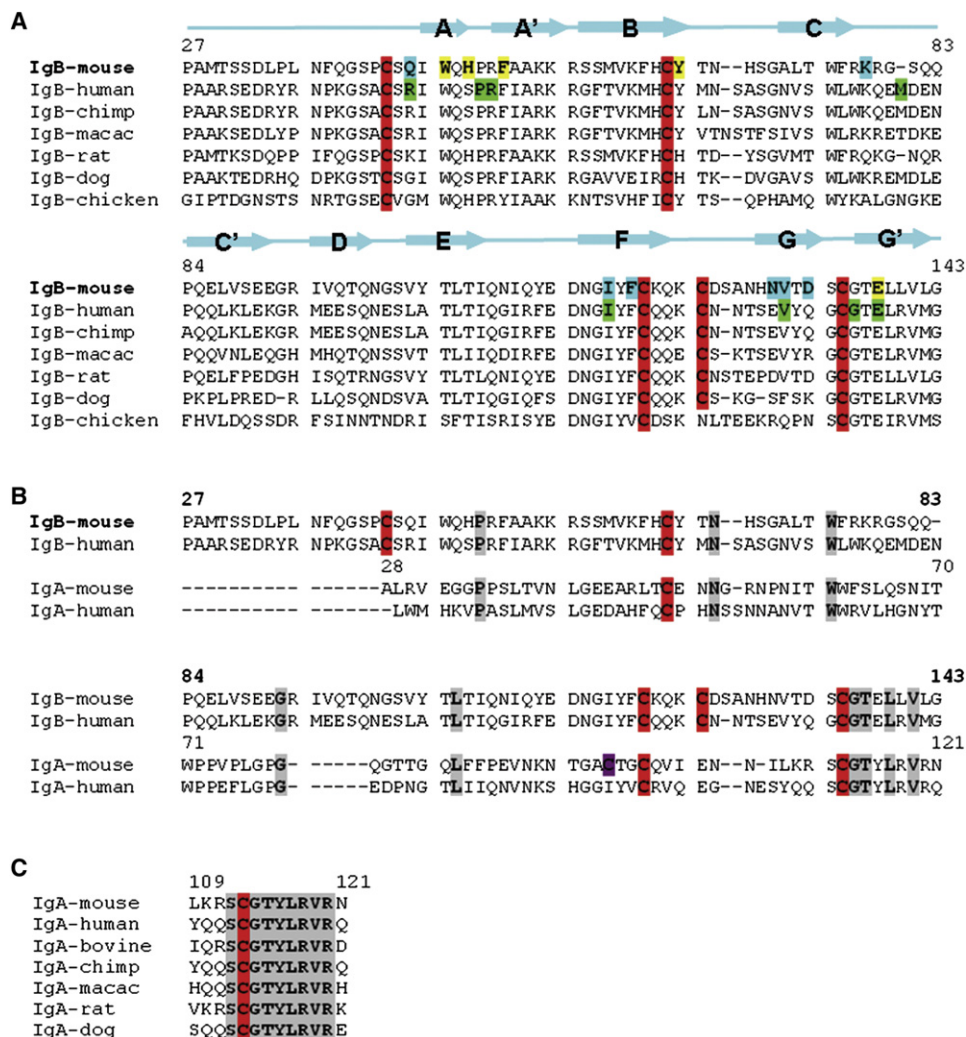


**Figure 4. Sequence Alignments of Igβs and Igαs**

(A) Sequence comparison of several mammalian and chicken Igβs. The numbering is consistent with the sequence of murine Igβ. The secondary-structure elements of Igβ are illustrated as arrows for β strands. Cysteines are highlighted red. Residues involved in interactions at the interface of the murine Igβ homodimer are highlighted according to subunit color, that is, cyan and yellow for A and B subunits, respectively. Residues involved in the interactions at the interface of human Igβ are highlighted green.

(B) Sequence alignment of murine and human Igβs and Igαs. The numbering is consistent with murine Igβ (bold font) and Igα (regular font). Cysteines are highlighted red. Unique cysteine 98 in murine Igα is highlighted magenta.

(C) Sequence alignment of several mammalian Igαs in the area of predicted G and G' strands. Conserved residues are highlighted gray. See also Figure S4.

bound to their respective antibodies in solution under experimental conditions. The mutational effects on BCR association were analyzed by solution binding experiments on immobilized Fcμ sensor chips. The wild-type Igα and Igβ exhibited similar binding affinities to immobilized Fcμ with dissociation constants  $K_D$  of ~1 μM, suggesting their equal contribution to μ chain association (Figure S5). The binding of Igα and Igβ mutants, reconstituted at 4 μM concentration in PBS, to Fcμ varied significantly depending on the mutations. In particular, three of the Igα mutants, H36A (α1), E85A (α4), and R124A/V125A/R126A (α5), resulted in 5- to 10-fold reductions in their binding to Fcμ compared to the wild-type. One mutation, N60A (α3) of Igα, exhibited a 2-fold increase in Fcμ binding (Figure 5C). Among the three mutants of human Igβ, R55A/K56A/R57A

(β1) and Q123A/Q124A/K125A (β4) each reduced their BCR binding by 6-fold and 2-fold, respectively, whereas K79A/Q80A/E81A (β3) increased binding moderately. First, the mutations further support the conclusion that both subunits of Igαβ are involved in BCR binding. Second, the mutations affecting Fcμ binding are broadly distributed rather than clustered on the surface of Igαβ. Third, the loss of Fcμ binding involves both positively and negatively charged residues, such as arginine and glutamate, suggesting significant electrostatic interactions present at the BCR and Igαβ interface. In addition, the location of these mutations and the size of Igαβ extracellular domain suggest the membrane proximal Cμ4 of BCR as the most likely contact domain for the extracellular domains of Igαβ heterodimer.

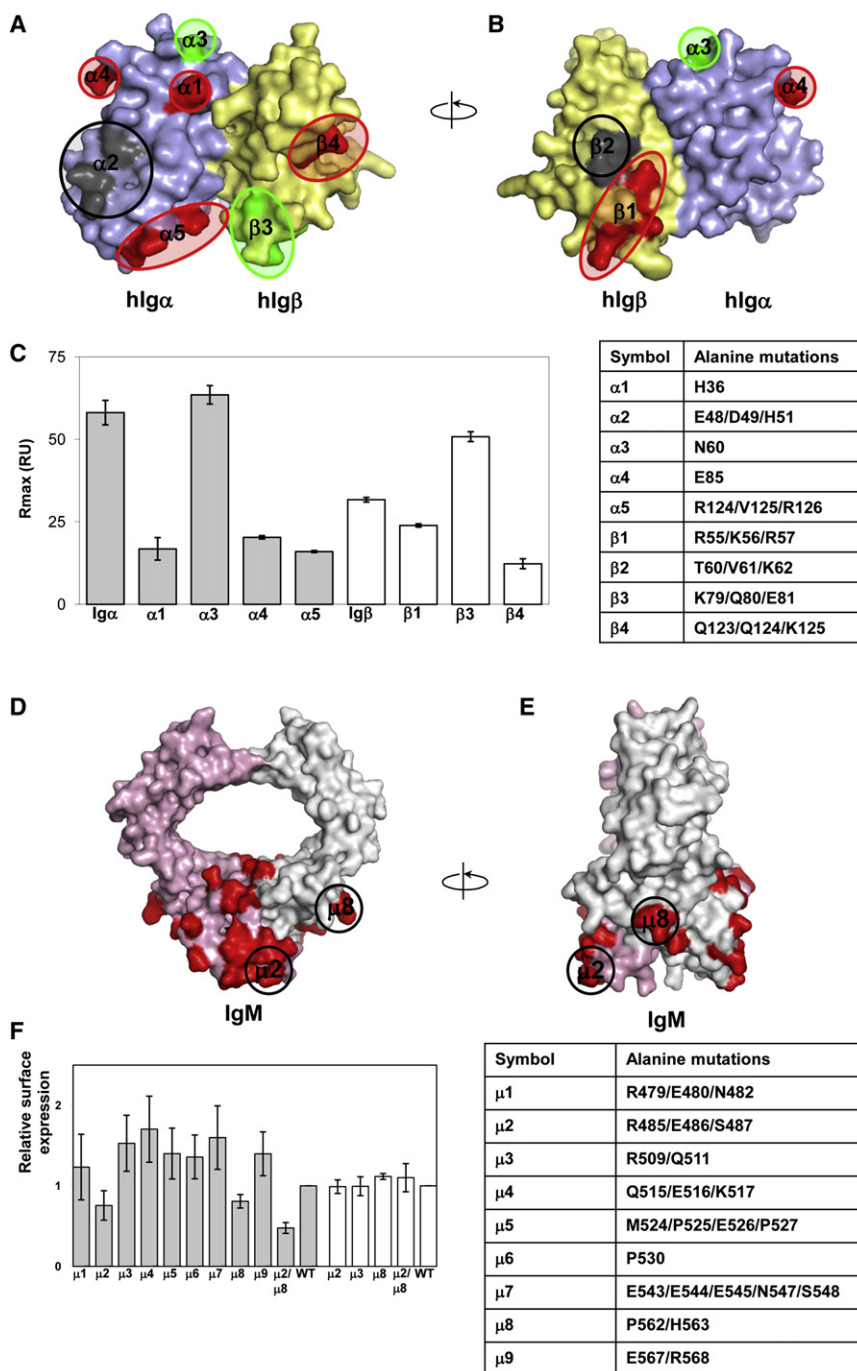


**Figure 5. Binding of Mutant Human Ig $\alpha$  and Ig $\beta$  to Recombinant Human C $\mu$ 2–C $\mu$ 4**

(A) Surface representation of human Ig $\alpha\beta$  heterodimer model. Point mutations resulting in reduction or increase of binding are circled red and green, respectively. Mutations causing absence of protein expression are circled black.  $\alpha$  and  $\beta$  chains of Ig $\alpha\beta$  heterodimer are colored pale blue and yellow, respectively.

(B) 180° rotation of the previous view of the Ig $\alpha\beta$  heterodimer model.

(C) Binding of Ig $\alpha$  (gray bars) and Ig $\beta$  (white bars) mutants to C $\mu$ 2–C $\mu$ 4. Mutant concentration in the analyte was kept constant at 4  $\mu$ M. At least three sets of experiments were performed for each mutant. A table with mutant description is given for reference.

(D) Structural model of C $\mu$ 3–C $\mu$ 4 domains of IgM. IgM chains are painted pink and gray with groups of amino acids selected for mutation in red. Groups of mutations  $\mu$ 2 (R485, E486, S487) and  $\mu$ 8 (P562, H563) that affect IgM surface expression are circled. Arginine 485 and proline 562 are highly conserved in IgM.

(E) 90° rotation of the previous view.

(F) Relative surface expression of different IgM groups of mutants (gray bars); white bars represent relative surface expression for IgM YS/VV construct. The YS/VV mutation in transmembrane domains of IgM allows surface IgM expression without binding to the Ig $\alpha\beta$  heterodimer. This indicates that the effects of the mutations were likely through disrupting interactions with Ig $\alpha\beta$ . A table with mutant descriptions is given for reference. See also Figure S5.

To investigate whether the C $\mu$ 4 domain of mIgM is involved in the binding to Ig $\alpha\beta$ , we used the mIgM surface expression on J558L cells to measure Ig $\alpha\beta$  association, as mIgM expression in this cell line is dependent on the assembly with Ig $\alpha\beta$  (Reth, 1992). A structural model of C $\mu$ 2–C $\mu$ 4 domains of mIgM was generated from the crystal structure of IgA to guide the selection of the mutational sites (Herr et al., 2003) (Figure 5). Based on this model, nine groups of amino acids (clusters  $\mu$ 1– $\mu$ 9) were selected evenly across the surface of C $\mu$ 4 for cluster mutational

analysis to probe the Ig $\alpha\beta$  contact site. Mutations were introduced into the B1-8 IgM heavy chain. Both the wild-type and mutant mIgM were transfected into J558L cells together with an Ig $\alpha$ -YFP plasmid, as J558L cells express endogenous Ig $\beta$  (Tolar et al., 2005). Whereas several cluster mutations mildly enhanced mIgM expression, two mutations, R485/E486/S487 ( $\mu$ 2) and P562/H563 ( $\mu$ 8), reduced surface expression of mIgM compared to that of the wild-type as determined by surface staining with anti-IgM antibodies (Figure 5F). Staining of permeabilized cells indicated that all mIgM constructs were present at similar levels intracellularly, suggesting variations in mIgM surface expression are not the result of transfection efficiency (Figure S5). Combined mutations of R485/E486/S487 ( $\mu$ 2) and P562/H563 ( $\mu$ 8) led to a further reduction in IgM surface expression without affecting intracellular levels of the IgM. The constructs were expressed normally when we introduced a YS/VV mutation into their transmembrane domains, which allows surface IgM expression without binding to the Ig $\alpha\beta$  heterodimer (Figure 5F), indicating that the effects of the mutations were likely



through disrupting interactions with Ig $\alpha\beta$ . Interestingly, residues in clusters  $\mu 2$  and  $\mu 8$  are conserved between human and mouse IgM but variable among other immunoglobulins. Importantly, residues affecting the association with Ig $\alpha\beta$  are spaced apart on the C $\mu 4$  domain, which is in accordance with our mutational studies on Ig $\alpha$  and Ig $\beta$ . Moreover, the IgM mutants with reduced binding to Ig $\alpha\beta$  also involve charged residues like Arg, His, and Glu, which again points to the probable electrostatic nature of interactions between BCR and Ig $\alpha\beta$ .

In summary, we determined the crystal structures of human and murine Ig $\beta$ . The structures adopt an Igl-like fold with a unique C' strand positioned across the  $\beta$  sandwich bridging the C and D strands. Both human and murine Ig $\beta$  form disulfide-bonded dimers through cysteines from their G strands that are distinct from the structures of existing Igl-like dimers. From the sequence conservation and hydrogen-bonding patterns, we modeled the Ig $\alpha\beta$  heterodimer structure based on the structure of the murine Ig $\beta$  dimer. Solution binding experiments using soluble Ig $\alpha\beta$  demonstrated a preferential recognition of  $\mu$  chain but not  $\alpha$ ,  $\gamma$ ,  $\delta$ , and  $\epsilon$  chains of BCR, suggesting a role for Ig $\alpha\beta$  to enhance BCR  $\mu$  chain signaling during B cell development and to compensate low antigen affinity of  $\mu$  chain. To define the contact region between  $\mu$  chain of BCR and extracellular domains of Ig $\alpha\beta$ , a series of cluster mutations was generated on Ig $\alpha$  and Ig $\beta$  as well as  $\mu$  chain of BCR. The binding analysis based on these cluster mutations showed an extensive contact surface between Ig $\alpha\beta$  and BCR involving both subunits of Ig $\alpha\beta$  through multiple charged residues.

## EXPERIMENTAL PROCEDURES

### Protein Expression and Purification

The extracellular portions of human Ig $\alpha$  (residues 33–143) and Ig $\beta$  (residues 26–159) and murine Ig $\beta$  (residues 27–159) were subcloned into a pET-30a vector using NdeI and XhoI restriction sites. Human Ig $\alpha$  and Ig $\beta$  mutants for binding studies were generated using the standard protocol with a Quik-Change kit (Stratagene). The recombinant proteins were expressed in *E. coli* BL21 (DE3) cells as inclusion bodies and then reconstituted in vitro similarly to previously described (Radaev et al., 2003). Human and mouse Ig $\beta$  showed a high tendency in forming disulfide-bonded homodimers; however, during murine Ig $\beta$  refolding, monomers with free cysteine blocked by glutathione were also observed. The renatured proteins were purified through an Ni-NTA affinity column followed by a size-exclusion column (Superdex 200; GE Healthcare). Purified proteins were dialyzed against the following buffers: murine Ig $\beta$  against 10 mM Na acetate (pH 5.2); human Ig $\beta$  against water; and human Ig $\alpha$  against 50 mM NaCl, 5 mM Tris (pH 9.0). The identity of the refolded proteins was confirmed by N-terminal amino acid sequencing, which showed some N-terminal degradation for murine Ig $\beta$ .

The extracellular domains of human and murine Ig $\alpha\beta$  fused with a leucine zipper (Ig $\alpha\beta$ -LZ) were expressed in insect cells using a similar procedure for both proteins. In brief, the extracellular portion of Ig $\alpha$  followed by a basic leucine zipper and a six-histidine tag was inserted into pBACp10p (Kozono et al., 1994) between XhoI and MroI sites. The extracellular part of Ig $\beta$  followed by an acidic leucine zipper and a FLAG tag was inserted into the same vector between EcoRI and SphI sites. A thrombin site was engineered between Ig $\alpha$  or Ig $\beta$  and the leucine zippers. The vector was cotransfected with BaculoGold linearized baculovirus DNA (Pharmingen) into sf9 cells. Recombinant virus was amplified and proteins were expressed in High Five cells cultured in Express Five SFM medium (Invitrogen) infected at a multiplicity of infection of 6. Ig $\alpha\beta$ -LZ was purified using an Ni-NTA affinity column followed by a size-exclusion Superdex 200 column. The Fc portion of a human BCR  $\mu$  chain (Fc $\mu$ , amino acid residues 258–586), corresponding to C $\mu 2$ –C $\mu 4$  regions, was expressed as a disulfide-bonded dimer in CHO cells. Total RNA of a human B

cell line, Daudi (American Type Culture Collection), was isolated using TRIZOL reagent (Invitrogen). The cDNA synthesis of a human membrane-bound form of IgM was performed utilizing a SuperScript First-Strand Synthesis System for RT-PCR kit (Invitrogen). Human Fc $\mu$  was PCR amplified from the cDNA using primers 5'-GGTTCTGCCTTTTCTCACCACCATCACCACCACCATCATA TTGCTGAGCTGCCTCCC-3' and 5'-CGGGATCCTCAGGTGGACCTTGTCAC GGTCC-3'. A second PCR was performed with primers 5'-AAAGGGGCTAG CGCCACCATGAAGTGGGTAACCTTCTCCTCCTC-3' and 5'-AGAAAAGGC AGAACCGGAGATGAAGAGGAGGAGAGAAAGTTAC-3' to insert a rat serum albumin leader sequence at the 5' end followed by a His $_8$  tag sequence. The segment was cloned into pIRES-neo3.0 plasmid (Clontech Laboratories), which was then stably transfected into CHO-lec3.2.8.1 cells (kindly provided by Dr. Pamela Stanley, Albert Einstein College of Medicine) using Lipofectamine 2000 (Invitrogen). G418-resisting clones were screened for Fc $\mu$  expression by ELISA and the clone with the highest expression level was selected for protein preparation. Conditioned CHO-S-SFM II spent medium containing Ig $\alpha\beta$ -LZ was collected using an Ni-NTA column and further purified on a Superdex 200 column.

### Crystallization and Structure Determination

Single crystals of the monomeric form of murine Ig $\beta$  were obtained by vapor diffusion in hanging drops at room temperature using reservoir solution containing 20% PEG 750MME, 0.2 M MgCl $_2$ , and 0.1 M sodium citrate (pH 5.0). Crystals of murine Ig $\beta$  homodimer grew in hanging drops with reservoir solution containing 0.72–1.0 M ammonium sulfate and 0.1 M Tris (pH 8.0–9.0), whereas the crystals of human Ig $\beta$  homodimer were obtained in 0.6 M Na formate and Na acetate (pH 4.0). The crystals of monomeric form of murine Ig $\beta$  diffracted to 1.7 Å, and contained one molecule per asymmetric unit. X-ray data sets were collected at the Southeast Regional Collaborative Access Team (SER-CAT) 22-ID beamline at the Advanced Photon Source, Argonne National Laboratory. Supporting institutions are listed at <http://www.ser-cat.org>. The data were processed and scaled with HKL2000 (Otwinowski and Minor, 1997). The structure was solved by molecular replacement using CNS v1.1 (Brunger et al., 1998). The polyaniline-based search model consisted of 70 core amino acids from the structure of TREM-1 (PDB ID code 1Q8M) that encompass portions of the B, C, D, E, F, and G  $\beta$  strands conserved among the V-type immunoglobulin structures. The program O was used for model building and adjustments (Kleywegt and Jones, 1997). Positional and individual B factor refinement was carried out using the maximum-likelihood target function of CNS v1.1 (Brunger et al., 1998), followed by REFMAC5 of the CCP4 program suite (CCP4, 1994; Murshudov et al., 1997). A well-defined glutathione molecule forming a disulfide bond to Cys124 was built into the electron density. The structure of the murine Ig $\beta$  homodimer was determined to 3.1 Å resolution by molecular replacement using the Ig $\beta$  monomer structure as a search model. The refinement and model building were done using programs CNS v1.1 and O, respectively. Two well-defined sulfate ions were located in the electron density map. The structure of human Ig $\beta$  homodimer was determined to 3.2 Å resolution using murine Ig $\beta$  monomer as the search model and refined using programs CNS v1.1 (Brunger et al., 1998), PHENIX.REFINE (Afonine et al., 2005), O (Kleywegt and Jones, 1997), and Coot (Emsley and Cowtan, 2004).

### Surface Plasmon Resonance

Human IgD (Calbiochem), human IgE, human IgA (Athens Research & Technology), human IgM, human IgG1  $\kappa$ , and human IgG1  $\lambda$  (Sigma) were purchased from commercial sources as indicated. Binding studies were performed with a BIAcore 3000 instrument and analyzed with BIAevaluation 4.1 software (Biacore AB). Recombinant Ig $\alpha\beta$  leucine zipper fusion proteins were immobilized individually onto a carboxymethylated dextran (CM5) chip using primary amine coupling in 10 mM sodium acetate (pH 4.5–5.5) at a flow rate of 10 ml/min to levels between 250 and 2000 response units (RU). The binding experiments were performed using serial dilutions of analytes in PBS buffer at a flow rate of 10 or 20  $\mu$ l/min. Only the binding experiments with Fc $\mu$  as analyte displayed good binding kinetics. The following antibodies were used as controls in binding studies: anti-human CD79a (clone JCB117; Lab Vision), anti-human CD79b (clone CB3-1; BD Biosciences), and anti-human IgM (Sigma). All recombinant proteins showed specific interactions with their corresponding antibodies. Surfaces were regenerated by brief



injection of either 10 mM NaOH or 10 mM glycine (pH 3.0). Dissociation constants ( $K_D$ ) were determined from either kinetic or steady-state fittings with BIAevaluation software. Binding studies on human Ig $\alpha$  and Ig $\beta$  mutants were performed in reverse orientation, where recombinant Fc $\mu$  was immobilized onto a CM5 chip using primary amine coupling in 10 mM sodium acetate (pH 5.0). Anti-human CD79a (clone JCB117; Lab Vision) and anti-human CD79b (clone CB3-1; BD Biosciences) antibodies were immobilized in separate flow cells on the same sensor chip to monitor the conformational integrity of mutant Ig $\alpha$  and Ig $\beta$ . The analytes consisted of individual mutants dissolved in PBS buffer at a constant concentration of 4  $\mu$ M. Similar binding affinities were obtained for the wild-type Ig $\alpha$  and Ig $\beta$  in this reverse immobilization. Surfaces were regenerated by brief injection of 5 mM NaOH and 5 mM glycine (pH 2.0). At least three sets of experiments were performed for each mutant.

### Cell-Surface Expression Analysis of IgM Mutants

The structure of C $\mu$ 3–C $\mu$ 4 domains of mouse IgM was modeled based on the structure of IgA (Herr et al., 2003). The nine clusters of surface residues of C $\mu$ 4 identified for alanine mutations were: R479/E480/N483 ( $\mu$ 1), R485/E486/S487 ( $\mu$ 2), R509/Q511 ( $\mu$ 3), Q515/E516/K517 ( $\mu$ 4), M524/P525/E526/P527 ( $\mu$ 5), P530 ( $\mu$ 6), E543/E544/E545/N547/S548 ( $\mu$ 7), P562/H563 ( $\mu$ 8), and E567/R568 ( $\mu$ 9). Mutations were introduced into B1-8 IgM heavy chain in pcDNA6 plasmid using a QuikChange kit (Stratagene). J558L cells were transiently cotransfected with the IgM constructs and Ig $\alpha$ -YFP using Amaxa electroporation as described (Tolar et al., 2005). After 36 hr, cells were fixed in paraformaldehyde, permeabilized or not with 0.1% Triton, and stained with anti-IgM-Cy5 (Jackson ImmunoResearch) antibodies. Surface expression was determined as mean fluorescence intensity of the IgM-positive cells normalized on the signal from IgM wild-type transfected cells.

### SUPPLEMENTAL INFORMATION

Supplemental Information includes five figures and can be found with this article online at doi:10.1016/j.str.2010.04.019.

### ACKNOWLEDGMENTS

We would like to thank Marina Zhuravleva and M. Gordon Joyce for their help in data collection. The use of the Advanced Photon Source was supported by the U.S. Department of Energy, Basic Energy Sciences, Office of Science, under contract W-31-109-Eng-38. This work is supported by intramural research funding from the National Institute of Allergy and Infectious Diseases.

Received: December 3, 2009

Revised: April 16, 2010

Accepted: April 21, 2010

Published: August 10, 2010

### REFERENCES

- Afonine, P.V., Grosse-Kunstleve, R.W., and Adams, P.D. (2005). A robust bulk-solvent correction and anisotropic scaling procedure. *Acta Crystallogr. D Biol. Crystallogr.* 61, 850–855.
- Alfarano, A., Indraccolo, S., Circosta, P., Minuzzo, S., Vallario, A., Zamarchi, R., Fregonese, A., Calderazzo, F., Faldella, A., Aragno, M., et al. (1999). An alternatively spliced form of CD79b gene may account for altered B-cell receptor expression in B-chronic lymphocytic leukemia. *Blood* 93, 2327–2335.
- Blum, J.H., Stevens, T.L., and DeFranco, A.L. (1993). Role of the  $\mu$  immunoglobulin heavy chain transmembrane and cytoplasmic domains in B cell antigen receptor expression and signal transduction. *J. Biol. Chem.* 268, 27236–27245.
- Brouns, G.S., de Vries, E., and Borst, J. (1995). Assembly and intracellular transport of the human B cell antigen receptor complex. *Int. Immunol.* 7, 359–368.
- Brunger, A.T., Adams, P.D., Clore, G.M., DeLano, W.L., Gros, P., Grosse-Kunstleve, R.W., Jiang, J.S., Kuszewski, J., Nilges, M., Pannu, N.S., et al. (1998). Crystallography & NMR system: a new software suite for macromolecular structure determination. *Acta Crystallogr. D Biol. Crystallogr.* 54, 905–921.
- Call, M.E., Pyrdol, J., Wiedmann, M., and Wucherpfennig, K.W. (2002). The organizing principle in the formation of the T cell receptor-CD3 complex. *Cell* 111, 967–979.
- Cambier, J.C. (1995). Antigen and Fc receptor signaling. The awesome power of the immunoreceptor tyrosine-based activation motif (ITAM). *J. Immunol.* 155, 3281–3285.
- Campbell, K.S., Hager, E.J., Friedrich, R.J., and Cambier, J.C. (1991). IgM antigen receptor complex contains phosphoprotein products of B29 and mb-1 genes. *Proc. Natl. Acad. Sci. USA* 88, 3982–3986.
- CCP4 (Collaborative Computational Project, Number 4). (1994). The CCP4 suite: programs for protein crystallography. *Acta Crystallogr. D Biol. Crystallogr.* 50, 760–763.
- Chothia, C., Gelfand, I., and Kister, A. (1998). Structural determinants in the sequences of immunoglobulin variable domain. *J. Mol. Biol.* 278, 457–479.
- Clevers, H., Alarcon, B., Wileman, T., and Terhorst, C. (1988). The T cell receptor/CD3 complex: a dynamic protein ensemble. *Annu. Rev. Immunol.* 6, 629–662.
- Cohen, G.H., Sheriff, S., and Davies, D.R. (1996). Refined structure of the monoclonal antibody HyHEL-5 with its antigen hen egg-white lysozyme. *Acta Crystallogr. D Biol. Crystallogr.* 52, 315–326.
- Dal Porto, J.M., Gauld, S.B., Merrell, K.T., Mills, D., Pugh-Bernard, A.E., and Cambier, J. (2004). B cell antigen receptor signaling 101. *Mol. Immunol.* 41, 599–613.
- Dylke, J., Lopes, J., Dang-Lawson, M., Machtaler, S., and Matsuuchi, L. (2007). Role of the extracellular and transmembrane domain of Ig- $\alpha/\beta$  in assembly of the B cell antigen receptor (BCR). *Immunol. Lett.* 112, 47–57.
- Emsley, P., and Cowtan, K. (2004). Coot: model-building tools for molecular graphics. *Acta Crystallogr. D Biol. Crystallogr.* 60, 2126–2132.
- Evans, E.J., Esnouf, R.M., Manso-Sancho, R., Gilbert, R.J., James, J.R., Yu, C., Fennelly, J.A., Vowles, C., Hanke, T., Walse, B., et al. (2005). Crystal structure of a soluble CD28-Fab complex. *Nat. Immunol.* 6, 271–279.
- Foy, S.P., and Matsuuchi, L. (2001). Association of B lymphocyte antigen receptor polypeptides with multiple chaperone proteins. *Immunol. Lett.* 78, 149–160.
- Garboczi, D.N., Ghosh, P., Utz, U., Fan, Q.R., Biddison, W.E., and Wiley, D.C. (1996). Structure of the complex between human T-cell receptor, viral peptide and HLA-A2. *Nature* 384, 134–141.
- Gauld, S.B., Dal Porto, J.M., and Cambier, J.C. (2002). B cell antigen receptor signaling: roles in cell development and disease. *Science* 296, 1641–1642.
- Geisberger, R., Lamers, M., and Achatz, G. (2006). The riddle of the dual expression of IgM and IgD. *Immunology* 118, 429–437.
- Grupp, S.A., Campbell, K., Mitchell, R.N., Cambier, J.C., and Abbas, A.K. (1993). Signaling-defective mutants of the B lymphocyte antigen receptor fail to associate with Ig- $\alpha$  and Ig- $\beta/\gamma$ . *J. Biol. Chem.* 268, 25776–25779.
- Grupp, S.A., Mitchell, R.N., Schreiber, K.L., McKean, D.J., and Abbas, A.K. (1995). Molecular mechanisms that control expression of the B lymphocyte antigen receptor complex. *J. Exp. Med.* 181, 161–168.
- Harpaz, Y., and Chothia, C. (1994). Many of the immunoglobulin superfamily domains in cell adhesion molecules and surface receptors belong to a new structural set which is close to that containing variable domains. *J. Mol. Biol.* 238, 528–539.
- Harris, L.J., Larson, S.B., Hasel, K.W., Day, J., Greenwood, A., and McPherson, A. (1992). The three-dimensional structure of an intact monoclonal antibody for canine lymphoma. *Nature* 360, 369–372.
- Hermanson, G.G., Eisenberg, D., Kincade, P.W., and Wall, R. (1988). B29: a member of the immunoglobulin gene superfamily exclusively expressed on  $\beta$ -lineage cells. *Proc. Natl. Acad. Sci. USA* 85, 6890–6894.
- Herr, A.B., Ballister, E.R., and Bjorkman, P.J. (2003). Insights into IgA-mediated immune responses from the crystal structures of human Fc $\alpha$ RI and its complex with IgA1-Fc. *Nature* 423, 614–620.

- Hombach, J., Tsubata, T., Leclercq, L., Stappert, H., and Reth, M. (1990). Molecular components of the B-cell antigen receptor complex of the IgM class. *Nature* 343, 760–762.
- Indraccolo, S., Minuzzo, S., Zamarchi, R., Calderazzo, F., Piovan, E., and Amadori, A. (2002). Alternatively spliced forms of Ig $\alpha$  and Ig $\beta$  prevent B cell receptor expression on the cell surface. *Eur. J. Immunol.* 32, 1530–1540.
- Jumaa, H., Hendriks, R.W., and Reth, M. (2005). B cell signaling and tumorigenesis. *Annu. Rev. Immunol.* 23, 415–445.
- Kashiwamura, S., Koyama, T., Matsuo, T., Steinmetz, M., Kimoto, M., and Sakaguchi, N. (1990). Structure of the murine mb-1 gene encoding a putative sIgM-associated molecule. *J. Immunol.* 145, 337–343.
- Kleywegt, G.J., and Jones, T.A. (1997). Model building and refinement practice. *Methods Enzymol.* 277, 208–230.
- Kozono, H., White, J., Clements, J., Marrack, P., and Kappler, J. (1994). Production of soluble MHC class II proteins with covalently bound single peptides. *Nature* 369, 151–154.
- Kuhns, M.S., Davis, M.M., and Garcia, K.C. (2006). Deconstructing the form and function of the TCR/CD3 complex. *Immunity* 24, 133–139.
- Lanier, L.L. (2005). NK cell recognition. *Annu. Rev. Immunol.* 23, 225–274.
- Leahy, D.J., Axel, R., and Hendrickson, W.A. (1992). Crystal structure of a soluble form of the human T cell coreceptor CD8 at 2.6 Å resolution. *Cell* 68, 1145–1162.
- Murshudov, G.N., Vagin, A.A., and Dodson, E.J. (1997). Refinement of macromolecular structures by the maximum-likelihood method. *Acta Crystallogr. D Biol. Crystallogr.* 53, 240–255.
- Nemazee, D., Kouskoff, V., Hertz, M., Lang, J., Melamed, D., Pape, K., and Retter, M. (2000). B-cell-receptor-dependent positive and negative selection in immature B cells. *Curr. Top. Microbiol. Immunol.* 245, 57–71.
- Ostrov, D.A., Shi, W., Schwartz, J.C., Almo, S.C., and Nathenson, S.G. (2000). Structure of murine CTLA-4 and its role in modulating T cell responsiveness. *Science* 290, 816–819.
- Otwinowski, Z., and Minor, W. (1997). Processing of X-ray diffraction data collected in oscillation mode. *Methods Enzymol.* 276, 307–326.
- Pleiman, C.M., Chien, N.C., and Cambier, J.C. (1994). Point mutations define a mIgM transmembrane region motif that determines intersubunit signal transduction in the antigen receptor. *J. Immunol.* 152, 2837–2844.
- Radaev, S., Kattah, M., Rostro, B., Colonna, M., and Sun, P.D. (2003). Crystal structure of the human myeloid cell activating receptor TREM-1. *Structure* 11, 1527–1535.
- Rajewsky, K. (1996). Clonal selection and learning in the antibody system. *Nature* 381, 751–758.
- Reth, M. (1989). Antigen receptor tail clue. *Nature* 338, 383–384.
- Reth, M. (1992). Antigen receptors on B lymphocytes. *Annu. Rev. Immunol.* 10, 97–121.
- Richardson, J.S. (1981). The anatomy and taxonomy of protein structure. *Adv. Protein Chem.* 34, 167–339.
- Schamel, W.W., and Reth, M. (2000). Monomeric and oligomeric complexes of the B cell antigen receptor. *Immunity* 13, 5–14.
- Schamel, W.W., Kuppig, S., Becker, B., Gimborn, K., Hauri, H.P., and Reth, M. (2003). A high-molecular-weight complex of membrane proteins BAP29/BAP31 is involved in the retention of membrane-bound IgD in the endoplasmic reticulum. *Proc. Natl. Acad. Sci. USA* 100, 9861–9866.
- Schwartz, J.C., Zhang, X., Fedorov, A.A., Nathenson, S.G., and Almo, S.C. (2001). Structural basis for co-stimulation by the human CTLA-4/B7-2 complex. *Nature* 410, 604–608.
- Siegers, G.M., Yang, J., Duerr, C.U., Nielsen, P.J., Reth, M., and Schamel, W.W. (2006). Identification of disulfide bonds in the Ig- $\alpha$ /Ig- $\beta$  component of the B cell antigen receptor using the *Drosophila* S2 cell reconstitution system. *Int. Immunol.* 18, 1385–1396.
- Tolar, P., Sohn, H.W., and Pierce, S.K. (2005). The initiation of antigen-induced B cell antigen receptor signaling viewed in living cells by fluorescence resonance energy transfer. *Nat. Immunol.* 6, 1168–1176.
- Venkitaraman, A.R., Williams, G.T., Dariavach, P., and Neuberger, M.S. (1991). The B-cell antigen receptor of the five immunoglobulin classes. *Nature* 352, 777–781.
- Wegener, A.M., Hou, X., Dietrich, J., and Geisler, C. (1995). Distinct domains of the CD3- $\gamma$  chain are involved in surface expression and function of the T cell antigen receptor. *J. Biol. Chem.* 270, 4675–4680.
- Wienands, J. (2005). Unraveling B cell receptor mechanics. *Nat. Immunol.* 6, 1072–1074.
- Williams, G.T., Peaker, C.J., Patel, K.J., and Neuberger, M.S. (1994). The  $\alpha/\beta$  sheath and its cytoplasmic tyrosines are required for signaling by the B-cell antigen receptor but not for capping or for serine/threonine-kinase recruitment. *Proc. Natl. Acad. Sci. USA* 91, 474–478.